



ARL-TR-8198 • Oct 2017



US Army Research Laboratory

# **Atmospheric Renewable Energy Research, Volume 4: Atmospheric Renewable Energy Field Study #2 (ARE2)**

**by Gail Vaucher, Jenna Forrester, Michael Curtice,  
Renea Young, Clayton Walker, and Sean D'Arcy**

Approved for public release; distribution is unlimited.

## **NOTICES**

### **Disclaimers**

The findings in this report are not to be construed as an official Department of the Army position unless so designated by other authorized documents.

Citation of manufacturer's or trade names does not constitute an official endorsement or approval of the use thereof.

Destroy this report when it is no longer needed. Do not return it to the originator.



# **Atmospheric Renewable Energy Research, Volume 4: Atmospheric Renewable Energy Field Study #2 (ARE2)**

**by Gail Vaucher and Sean D’Arcy**

*Computational and Information Sciences Directorate, ARL*

**Jenna Forrester**

*Advanced Individual Academic Development Internship, US Military Academy*

**Michael Curtice**

*Thurgood Marshall College Fund Internship, Central State University*

**Renea Young**

*Thurgood Marshall College Fund Internship, Mississippi Valley State University*

**Clayton Walker**

*Reserve Officers’ Training Corps Internship, Embry Riddle Aeronautical University*

**REPORT DOCUMENTATION PAGE**

*Form Approved  
OMB No. 0704-0188*

Public reporting burden for this collection of information is estimated to average 1 hour per response, including the time for reviewing instructions, searching existing data sources, gathering and maintaining the data needed, and completing and reviewing the collection information. Send comments regarding this burden estimate or any other aspect of this collection of information, including suggestions for reducing the burden, to Department of Defense, Washington Headquarters Services, Directorate for Information Operations and Reports (0704-0188), 1215 Jefferson Davis Highway, Suite 1204, Arlington, VA 22202-4302. Respondents should be aware that notwithstanding any other provision of law, no person shall be subject to any penalty for failing to comply with a collection of information if it does not display a currently valid OMB control number.

**PLEASE DO NOT RETURN YOUR FORM TO THE ABOVE ADDRESS.**

<b>1. REPORT DATE (DD-MM-YYYY)</b> October 2017		<b>2. REPORT TYPE</b> Technical Report		<b>3. DATES COVERED (From - To)</b> 31 May 2017–30 September 2017	
<b>4. TITLE AND SUBTITLE</b> Atmospheric Renewable Energy Research, Volume 4: Atmospheric Renewable Energy Field Study #2 (ARE2)				<b>5a. CONTRACT NUMBER</b>	
				<b>5b. GRANT NUMBER</b>	
				<b>5c. PROGRAM ELEMENT NUMBER</b>	
<b>6. AUTHOR(S)</b> Gail Vaucher, Jenna Forrester, Michael Curtice, Renea Young, Clayton Walker, and Sean D'Arcy				<b>5d. PROJECT NUMBER</b>	
				<b>5e. TASK NUMBER</b>	
				<b>5f. WORK UNIT NUMBER</b>	
<b>7. PERFORMING ORGANIZATION NAME(S) AND ADDRESS(ES)</b> US Army Research Laboratory Computational and Information Sciences Directorate: Battlefield Environment Division (ATTN: RDRL-CIE-D) White Sands Missile Range, NM 88002-5501				<b>8. PERFORMING ORGANIZATION REPORT NUMBER</b>  ARL-TR-8198	
<b>9. SPONSORING/MONITORING AGENCY NAME(S) AND ADDRESS(ES)</b>				<b>10. SPONSOR/MONITOR'S ACRONYM(S)</b>	
				<b>11. SPONSOR/MONITOR'S REPORT NUMBER(S)</b>	
<b>12. DISTRIBUTION/AVAILABILITY STATEMENT</b> Approved for public release; distribution is unlimited.					
<b>13. SUPPLEMENTARY NOTES</b>					
<b>14. ABSTRACT</b> Harvesting energy from local resources (such as the sunlight) and integrating these into traditional microgrids is one way to establish tactical power grid independence. Traditional generators have an optimum setting for maximizing fuel economy. Coupling these generators with solar power requires anticipating and exploiting ideal atmospheric contributions that best match the traditional generator's optimum operating requirements. This ideal was the goal behind the Atmospheric Renewable Energy Field Study #2 (ARE2). ARE2 has produced a novel and detailed power, solar radiation, and cloud/sky documentation data set. The potential services provided by the data set range from basic research seeking to investigate improved understanding of cloud impacts on solar radiation to practical research applications that seek to develop algorithms to empower diagnostic and predictive solar radiation tools tailored specifically for grid power production. This report was written to establish a common starting point for those seeking to use and exploit this data set.					
<b>15. SUBJECT TERMS</b> atmospheric renewable energy, ARE2, solar radiation, clouds, simulated Whole Sky Imager, sWSI, Power Train					
<b>16. SECURITY CLASSIFICATION OF:</b>			<b>17. LIMITATION OF ABSTRACT</b>  UU	<b>18. NUMBER OF PAGES</b>  30	<b>19a. NAME OF RESPONSIBLE PERSON</b> Gail Vaucher
<b>a. REPORT</b> Unclassified	<b>b. ABSTRACT</b> Unclassified	<b>c. THIS PAGE</b> Unclassified			<b>19b. TELEPHONE NUMBER (Include area code)</b> (575) 678-3237

## Contents

---

<b>List of Figures</b>	<b>v</b>
<b>List of Tables</b>	<b>v</b>
<b>Acknowledgments</b>	<b>vi</b>
<b>Executive Summary</b>	<b>vii</b>
<b>1. Introduction</b>	<b>1</b>
1.1 Long-Term Vision	1
1.2 Atmospheric Impacts on Solar Power	2
1.3 Tactical Energy Unit Independence	2
1.4 ARE2 Test Plan	2
<b>2. Field Study (ARE2)</b>	<b>3</b>
2.1 ARE2 Preparations	3
2.2 ARE2 Schedule	3
2.3 ARE2 Field Design	4
2.3.1 Power Train	4
2.3.2 Quantifying the Atmosphere	5
<b>3. ARE2 Data Acquisition and Preliminary Data Processing</b>	<b>6</b>
3.1 Power Train Data Acquisition and Processing	6
3.2 Solar Radiation Data Acquisition	8
3.3 Preliminary Processing of Power and Pyranometer Data	9
3.4 Sky/Cloud Data Acquisition	10
3.5 Sky/Cloud Data Processing	11
<b>4. Results and Discussion</b>	<b>13</b>
4.1 Observations from the sWSI Data	13
4.2 Lessons Learned	15

<b>5. Conclusion and Recommendations</b>	<b>16</b>
<b>6. References</b>	<b>17</b>
<b>List of Symbols, Abbreviations, and Acronyms</b>	<b>18</b>
<b>Distribution List</b>	<b>20</b>

## List of Figures

---

---

Fig. 1	a) ARE2 and b) Local-Rapid Evaluation of Atmospheric Conditions (L-REAC) systems.....	4
Fig. 2	ARE2 Power Train major elements .....	6
Fig. 3	ARE2 Power Train design .....	7
Fig. 4	ARE2: 2017 June 18, clear sky case.....	9
Fig. 5	Examples of over, under, and balanced exposures taken from the sWSI, with artificial intensity histogram profiles .....	10
Fig. 6	sWSI digitization example.....	13

## List of Tables

---

---

Table 1	sWSI digitization categories examples .....	12
---------	---	----

## **Acknowledgments**

---

The authors wish to thank Tim Chavez for his generous and timely help in addressing the Power Train issues, and Robert Brice for his help with the initial pyranometer setup. Also, special thanks go to the Technical Publishing Branch for its technical editing excellence, specifically to Jessica Schultheis, Lisa Lacey, and Amber Bennett.

## Executive Summary

---

Harvesting energy from locally available resources is one way to establish tactical power grid independence. Integrating renewable energy resources into traditional microgrids reduces the hazards associated with fuel requirements, which in turn reduces fiscal costs, lowers logistical risks, and provides a more diversified power resource. The net effect is a more agile and less burdened tactical field unit.

Hybridizing traditional grid resources with solar (or wind) power requires knowledge of atmospheric impacts on these renewable energy commodities. For this report, we focus on solar power, gleaned from photovoltaic (PV) technology, as the renewable energy resource. Exploiting atmospheric contributions to the solar power can lead to more optimized efficiency and effectiveness for the hybrid microgrid. One might presume that having more sun reach the PV panels would result in more power from the panels and create an ideal scenario for a hybrid power grid. In reality, however, traditional generators have an optimum setting for maximizing fuel economy. The initial hybrid engineers targeted this setting for optimizing grid efficiency. Consequently, the desired atmospheric contribution changes from identifying the maximum amount of solar input to anticipating (forecasting) and exploiting current solar input that best matches the traditional generator's optimum operating requirements. The forecasted solar radiation status could strengthen the Distributed Grid Manager function. Knowing and exploiting the current atmospheric conditions could better assist the Distributed Model Based Control in its optimizing routines. Such atmospheric intelligence skills redefine the needed atmospheric understanding. It was around these revised requirements that the Atmospheric Renewable Energy Field Study #2 (ARE2) was designed.

In this report, we describe the field study hardware, data acquisition, and preliminary data processing. The report concludes with a summary of observations and lessons learned. ARE2 has produced a novel and detailed power, solar radiation, and cloud/sky documentation data set. The potential services provided by these data range from basic research seeking to investigate improved understanding of cloud impacts on solar radiation to practical application research that seeks to develop complex algorithms to empower diagnostic and predictive solar radiation tools tailored specifically for grid power production. This report was written to establish a common starting point for those seeking to use and exploit this data set. It is recommended that users of the data continue to document their findings so that the seeds planted can continue to grow into new understandings.

INTENTIONALLY LEFT BLANK.

## **1. Introduction**

---

Establishing tactical power grid independence has the potential for providing a significant strategic military advantage for remote location missions, operations, and logistics. One method for power grid independence is through the harvesting of energy from locally available resources. Integrating renewable energy resources into traditional microgrids reduces the hazards associated with fuel requirements, which in turn reduces fiscal costs, lowers logistical risks, and provides a more diversified power resource. The net effect is a more agile and less burdened tactical field unit (Vaucher 2015).

Hybridizing traditional grid resources with solar (or wind) power requires knowledge of atmospheric impacts on these renewable energy commodities. For this report, we focus on solar power as the renewable energy resource. Exploiting atmospheric contributions to solar power can lead to more optimized efficiency and effectiveness for the hybrid microgrid. Presuming solar energy is being extracted using photovoltaic (PV) panels (versus solar thermal collection), one would naturally presume that having more sun reach the PV panels would generate more power from the panels, and create an ideal scenario for a hybrid power grid. In reality, however, traditional generators have an optimum setting for maximizing fuel economy. This setting reduces generator fuel requirements and ultimately optimizes grid efficiency that the initial hybrid engineers are seeking. Consequently, the desired atmospheric ambition changes from identifying the maximum amount of solar input to anticipating (forecasting) and exploiting current solar input that best matches the traditional generator's optimum operating requirements. The forecasted solar radiation status could strengthen the Distributed Grid Manager (DGM) function, which is to anticipate power supply and load demands. Knowing and exploiting the current atmospheric conditions could better assist the Distributed Model Based Control (DMBC) in its power grid optimizing routines. Such atmospheric intelligence skills redefine the needed atmospheric understanding. It is around these revised requirements that the Atmospheric Renewable Energy Field Study #2 (ARE2) was designed.

### **1.1 Long-Term Vision**

---

The long-term vision motivating the ARE studies is to package the atmospheric intelligence into useful terms and quantities for microgrid applications. Successfully completing this goal requires understanding both the atmosphere and power microgrids. Practical hands-on experience gained from the physical construction and maintaining of the ARE2 Power Train, as well as work in

simulating various microgrid functions under predetermined atmospheric conditions, significantly enhanced and refined the vision into its current pioneering optimization goals. As this project evolves, we hope to continue refining the end-target, until a truly lean and proficient communication of atmospheric quantities are defined and proven for hybrid microgrid applications.

## **1.2 Atmospheric Impacts on Solar Power**

---

In ARE Research, Volume 3 (Vaucher et al. 2016), the 2 primary atmospheric contributions were defined as solar radiation and ambient temperature. The major inhibitors of solar radiation traversing from space to the PV panels on or near the earth's surface were categorized as hard and soft shadows. The hard shadows included those from building structures, fallen branches, growing plants, and so on. The soft shadows were caused by clouds and aerosols/dust. Since most hard shadows can be mitigated through design/configuration choices, ARE2 focused on quantifying the soft shadows. This topic will be expanded on in Section 3.

The impact of ambient temperature on solar power generation is primarily associated with system efficiency. The ambient temperature used for PV panel calibration of "peak power" is 25 °C. For every 1 °C above (or below) the calibration ambient temperature, the solar power system will lose (or gain) a 0.5% efficiency (Boxwell 2013). Consequently, when temperatures are extremely warm, the system's efficiency drops. When temperatures are colder, efficiency improves with respect to the panel's peak power.

## **1.3 Tactical Energy Unit Independence**

---

Power grids that truly function independently carry the additional criteria that all input resources need to be isolated from the outside environment. This restriction is one of the major features that distinguish this research from work done by other agencies (Haupt et al. 2016). The self-imposed limitation had a major influence on the ARE2 study data acquired, the acquisition design, and the final model application resources.

## **1.4 ARE2 Test Plan**

---

The primary ARE2 goal was to acquire data that would assess the atmospheric impact on PV power generation for isolated hybrid microgrids. The measurements selected included data that would document and quantify the general surface layer atmospheric conditions, the sky/cloud conditions, and the concurrent PV power generation. The data usages were designed to be multifunctional. One vision was to use data to empirically confirm and/or derive links between surface solar

radiation and cloud types, cloud amounts, and/or PV power out. Another task was to pursue these correlations through the use of machine learning techniques. This latter method would require the additional step of digitizing the sky documentation, thus enabling machines to learn cloud characterization from image documentation.

The ARE2 design and data types will be described in the following sections.

## **2. Field Study (ARE2)**

---

---

ARE2 was conducted in a southwestern USA desert location. The data were acquired from the roof of a 2-story building at White Sands Missile Range, New Mexico. The location is geographically situated on the west side of an approximately 40-mile-wide, relatively flat basin called the Tularosa Basin. Jagged mountains along the west side of the Tularosa Basin rise to about 8,000 ft. Relatively flat-topped mountains to the east rise about 10,000 ft, with a single mountain peak of 12,000 ft to the northeast.

### **2.1 ARE2 Preparations**

---

Several pretests and a calibration test were conducted prior to the actual ARE2 execution. The net results of the pretests were to identify and replace bad sensors/equipment, test the data acquisition and support software, and establish and refine sky documentation skills/techniques. A relative calibration (side-by-side) of sensors was executed just prior to the actual field study start. The preliminary calibration results, while not formalized, were sufficient for initiating the study.

### **2.2 ARE2 Schedule**

---

ARE2 was purposely scheduled to occur during the 2 summer months of June and July. Due to questionable power data, the data acquisition duration was extended into early August. The summer month selection was based on the southwestern desert weather patterns of clear skies in June and partly cloudy-to-overcast skies in July. The clear sky and overcast conditions were chosen to provide 2 anchoring reference points for correlating sky and power generation. The random nature of the partly cloudy cases were sought to fill in the many variations needed to challenge future atmospheric model/power-output algorithms development.

## 2.3 ARE2 Field Design

---

The general ARE2 design consisted of 3 major elements: Power Train, in situ atmospheric measurements, and regional weather summaries. The hardware associated with each element will be described in the following sections. An overview of the element's data acquisition methods is presented in Section 3.

### 2.3.1 Power Train

The ARE2 hardware design is shown in Figs. 1a and 1b. The Power Train design included a 72-cell SolarWorld (Sunmodule SW 315 XL Mono) solar PV panel. This single panel faced south and was tilted at an angle of about  $32^\circ$ , the approximate latitude of the site. Optimum solar photon intake occurs when the photons arrive orthogonally (at  $90^\circ$ ) to the panel plane (Vaucher 2016), as shown in Fig. 1. The panel had a rated max power of 315 W (-0/+5 Wp) and a maximum system voltage of 1000 V DC. The rated voltage was 36.8 V and the rated current was 8.63 A.

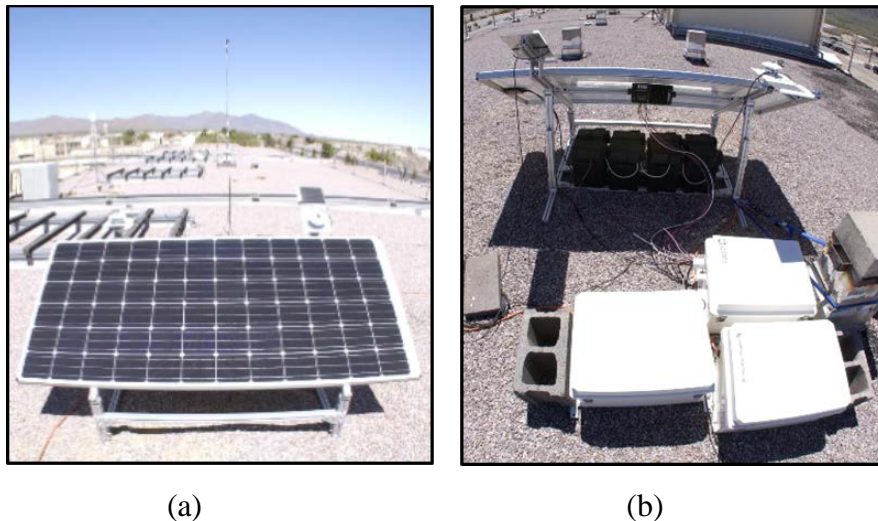


**Fig. 1** a) ARE2 and b) Local-Rapid Evaluation of Atmospheric Conditions (L-REAC) systems

Electrical power generated from the panel went through a 30-A Maximum Power Point Tracking (MPPT) Charge Controller (MidNite Solar, Model “the Kid”). Four Trojan T105re (renewable energy) deep-cycle flooded lead acid batteries were charged by the controller, which assimilated the sun-generated PV panel output. A BK Precision 8510 Programmable DC Electronic (Digital) Load was included to balance the electrical flow in the ARE2 Power Train.

The function of the battery was to either absorb or discharge power, depending on whether the panel was taking in sunlight. The Digital Load's function was strictly to absorb power. The MPPT controller regulated the power between the 2 elements.

The manual method for balancing the Power Train consisted of evaluating the digital load voltages in the morning and evening. For the ARE2 configuration, the ideal load values were greater than 22 V in the morning, and less than 25 V in the evening. Amperage was manually adjusted based on these empirical guidelines. When morning voltage showed signs of dropping below 22 V, the load amperage was reduced to let the batteries charge. When the evening voltage exceeded 25 V, the load was increased, which then brought the voltage down.

## **2.3.2 Quantifying the Atmosphere**

Atmospheric conditions were documented using in situ measurements and regional weather summaries. The in situ measurements consisted of a standard atmospheric parameterization and 2 solar radiation sensors. The following sections will elaborate on each element.

### **2.3.2.1 Standard Atmospheric Measurements**

The in situ atmospheric description was provided by the Local-Rapid Evaluation of Atmospheric Conditions (L-REAC) system located due north, on the same roof as the ARE2 System. The L-REAC system tower is in the center of Fig. 1a. The physical separation of the 2 systems was about 16 m. The variables sampled by the L-REAC included pressure (1 m above roof level [ArL]), 2 temperatures (5.7 m and 0.7 m ArL), relative humidity (2 m ArL), wind speed/wind direction (6 m ArL), and solar radiation (2 m ArL). These measurements were sampled every 10 s and reduced to a 1 min average. For more detailed information, see L-REAC system (Vaucher et al. 2011).

### **2.3.2.2 Solar Radiation Measurements**

In situ solar radiation measurements were taken by 2 Kipp/Zonen Model CM3 pyranometers sampling every 10 s, in watts per square meter ( $\text{W}/\text{m}^2$ ), and calculating 1 min averages. Each pyranometer was mounted on a flat plate that was attached to the top of the PV panel. Pyranometer #1-West (140328) was mounted on the northwest corner of the PV panel (approximately 1.05 m ArL); Pyranometer #2-East (140323) was attached to the northeast corner of the PV panel at the same height ArL. For the calibration test, both platforms were positioned parallel to the ground, giving the sensor a  $360^\circ$  horizontal range and a  $180^\circ$  zenith field of view (fov). Once that test was completed, the eastern pyranometer (#2) was reorientated to the angle of the south-facing PV panel, approximately  $32^\circ$  (1.03 m ArL). The impacts of the angled perspective are demonstrated in Section 3.

### 2.3.2.3 Sky Documentation

Documenting the sky conditions required 3 steps: acquiring an image from the simulated Whole Sky Imager (sWSI), logging a cloud observation within minutes of the sWSI image, and extracting online, automated observations from a nearby Air Force Base archive.

The sWSI consisted of a Professional NIKON D750 camera with a Sigma 8mm 180° fisheye lens. The sky observations followed a standard 3-tiered (high, middle, low layer) sky observation process, coupled with an automated weather sensor within 40 miles of the ARE2 field site. The method for documenting the sky/cloud conditions will be described in Section 3.4.

## 3. ARE2 Data Acquisition and Preliminary Data Processing

This section describes the ARE2 power and atmospheric data acquisition methods and preliminary data processing.

### 3.1 Power Train Data Acquisition and Processing

The major Power Train elements are shown in Fig. 2. These include the PV panel, controller, batteries, and a digital load. Samples of current and voltage were taken in 3 locations: 1) between the PV panel and controller (PV Power), 2) between the controller and battery (battery power), and 3) between the controller and load (load power).

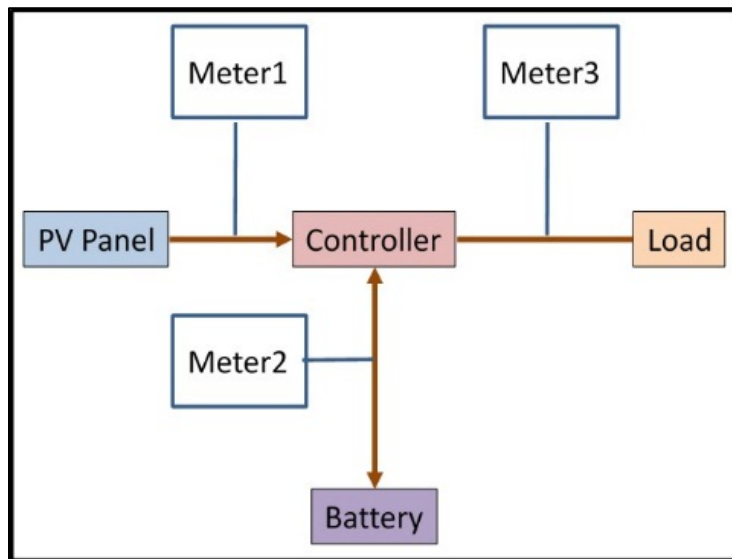


Fig. 2 ARE2 Power Train major elements

The current/voltage samples were taken near the circuit breaker at a rate of 25 samples/5 s (Fig. 3). Hourly files of these data were automatically preserved by the US Army Research Laboratory (ARL)-designed Labview data acquisition system (DAS). The hourly files were merged into a single-day data file and the resulting data file was used for assessing the data.

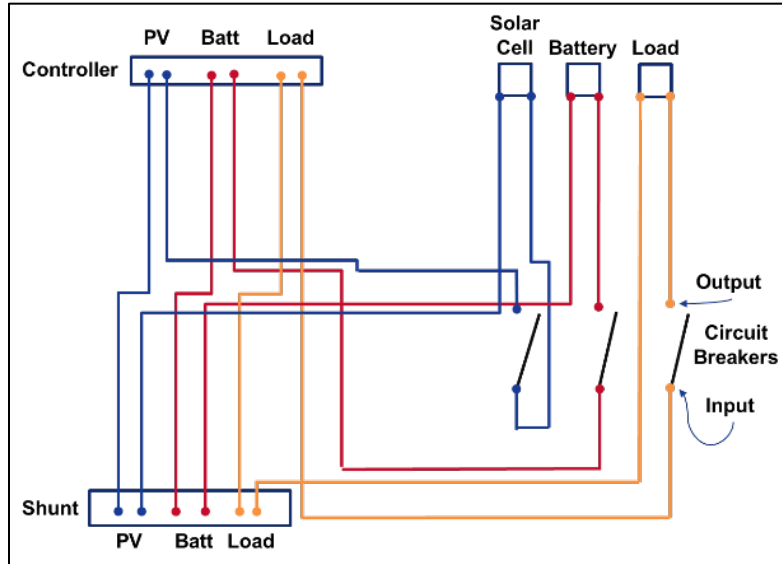


Fig. 3 ARE2 Power Train design

To access data quality, hourly power data files were removed from the DAS in a quasi-daily routine. These files were combined into a single 24 h (1 d) data file. The current (I) and voltage (V) samples were reduced to 1-min averages. Power (P) was then calculated using the standard power equation of

$$P = I * V. \quad (1)$$

In this equation, voltage is measured in volts, current in amps, and power in watts. If current (amperage) was not available, but resistance was obtainable, then one could have used

$$\text{Power} = \text{Current}^2 * \text{Resistance (Ohms)}. \quad (2)$$

This equation was derived from the fact that voltage is a product of current and resistance, or  $V = I * R$ . Substituting this into power from Eq. 1:

$$P = I * (I * R) \quad (3)$$

$$P = I^2 * R. \quad (4)$$

For the routine ARE2 daily power data assessments, only Eq. 1 was required. Power output plots were reviewed for quality control purposes by the Power Train designer.

The ARE2 power, solar radiation, and sWSI data were preserved on a CD and transferred to an archive for future analyses.

### **3.2 Solar Radiation Data Acquisition**

---

Pyranometer data from the ARE2 and L-REAC systems were reviewed on a daily basis. During the main field study there were a total of 3 pyranometers acquiring data, 24 h/d, 7 d/week (24/7). Two sensors sampled from a zenith fov and one from an angled fov. Unlike the ARE2 pyranometers, which sampled at about 1 m ArL, the L-REAC pyranometer sampled data at 2 m ArL.

During clear sky days, a preliminary data assessment between pyranometers could be done. Figure 4 shows such a case for June 18, 2017. In this midnight-to-midnight time series, the peak solar radiation values for the angled sensor exceeded the zenith fov sensor, as expected. Direct solar radiation impacts the PV panel more intensely than when the panel is off-axis (such as having a zenith fov) with the solar position. The signature smooth time series curve was consistent between the 2 sensors. The few random dips were a result of human and/or known structure shadows.

Intuitively, one would expect peak solar radiation to occur midday when the sun's elevation is at a maximum. In Fig. 4, the peak values are logged about an hour later. This timing is due to data being time stamped in local time values, which for June in New Mexico is Mountain Daylight Time (MDT). Consequently, the maximum values occur at 1307–1309 MDT, an hour different from “sun time”, which is based on solar elevation angle.

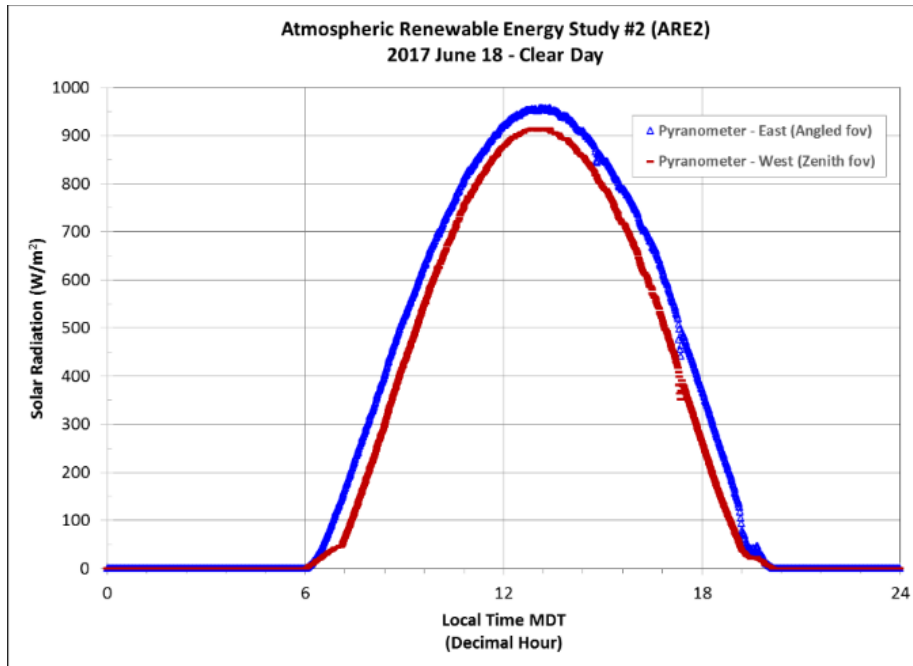


Fig. 4 ARE2: 2017 June 18, clear sky case

### 3.3 Preliminary Processing of Power and Pyranometer Data

Power Train and solar radiation data were concurrently retrieved and a preliminary evaluation was executed daily. Linking these 2 independently acquired measurement resources required time stamp synchronization. The process for doing this action was as follows.

First, the time stamps of the Power, Pyranometer and sWSI data acquisition systems were observed and documented. The “true” time stamp was taken each morning, from a NIKON GP-1a GPS device attached to the sWSI. This device linked to 3–4 satellites. Once locked in, the sWSI time-stamp display was used to update the Inspiron DAS computer clock. The Inspiron laptop contained the Pyranometer Campbell Scientific PC200W 4.3 software used to download solar radiation data files. Bringing the time-synched Inspiron DAS to the roof, the automated CR6 data-logger was connected. Using a PC200W software function, both the Inspiron and CR6 time stamps were displayed. These values were documented in the daily ARE2 field logbook. The pyranometer data were then downloaded. If a time difference of more than 5 s was noted, the CR6 time was resynchronized with the GPS-calibrated Inspiron clock and the update was noted in the logbook.

The Labview-Power Train DAS program copied its time stamp from the resident DAS computer, which was automatically updated using a second GPS device. A comparison between DAS clocks (Inspiron and Power DAS) was noted and logged.

### 3.4 Sky/Cloud Data Acquisition

The sWSI consisted of a Professional NIKON D750 camera with a Sigma 8mm 180° fisheye lens. Using no solar occulting device, whole sky images were taken on the same platform and orientation as each ARE2 pyranometer. With careful attention taken regarding the exposure, details of sky and clouds were preserved on digital film for later analyses. Figure 5 provides examples of an overexposed image, an underexposed image, and the ideal balanced exposure needed for the sWSI data. The sWSI sensor automatically provided an intensity (range of brightness) histogram of the image taken (Nikon 2014). After persistent experimentation with exposure compensation, it was found that when the histogram reported slightly underexposed values (histogram peak was slightly left of center), then the details of the sky and clouds would be most readily discerned. Figure 5 uses typical exposure values of  $\pm 1.5$  to demonstrate the concept.

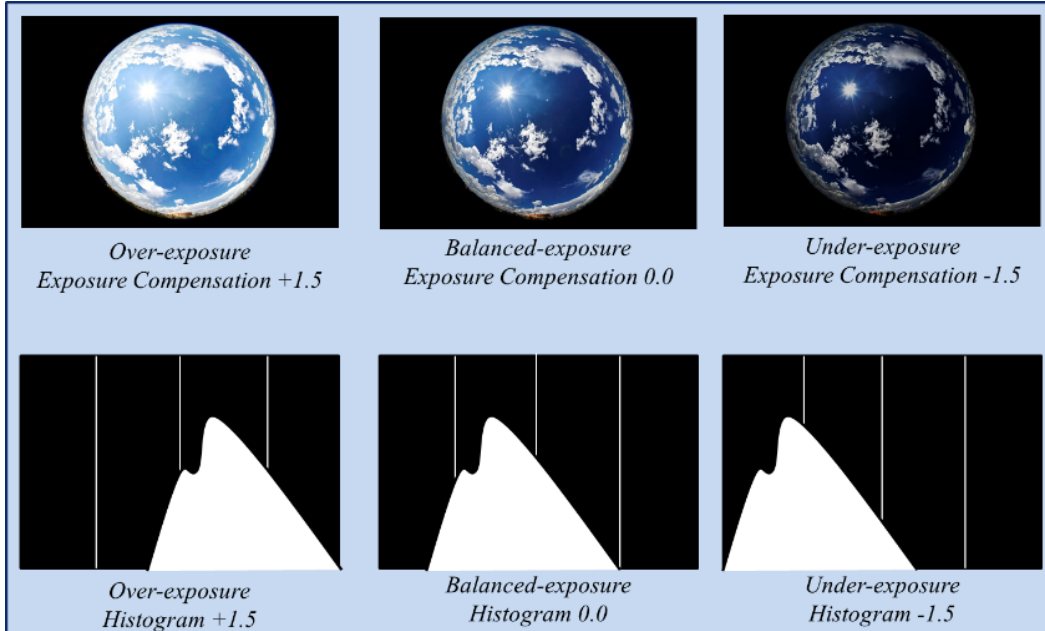


**Fig. 5** Examples of over, under, and balanced exposures taken from the sWSI, with artificial intensity histogram profiles

Unlike the original ARE1 NIKON D1X sWSI, the output of this sWSI was not limited by an image crop sensor. Only 1 image was required to capture the entire sky. For ARE2, the sWSI data were manually acquired on an hourly basis between 0800 and 1600 MDT, during most business days.

Within minutes of the sWSI image acquisition, the observer documented sky conditions. This documentation began by first noting whether the sun was obscured by cloud cover. Then, the observer subdivided the description into 3 layers: high,

middle, and low cloud layers. Using an *Aerographer's Mate Third Class Observer Manual* and NOAA/NASA cloud standards, up to 9 potential cloud types were reported (Naval Education and Training Program Development Center 1984, NOAA/NASA 2015). The high layer clouds included cirrus cloud types: cirrostratus (Cs), cirrocumulus (Cc), and cirrus (Ci). Mid-layer clouds consisted of altostratus (As) and altocumulus (Ac). The low layer clouds included stratus (St) and various cumulus clouds (stratocumulus [Sc], cumulonimbus [Cb], and cumulus [Cu]). Special provisions were made for the presence of smoke and fog, as well as the atypical (for summertime) desert nimbostratus (Ns) clouds.

Each documented layer included a quantity descriptor scaled by tenths. When the sky was clear, 0/10 was recorded. For overcast sky, 10/10 was noted. If the top layer had 50% of the sky covered with Ci, then 5/10 was marked in the "Top" layer box of the observation table. For each hourly data acquisition, the sWSI image specifications and the observed cloud conditions were manually transcribed into a table for future analyses.

The online, automated observations from a nearby Air Force Base were archived each business day. This resource represented a sky view that was about 40 miles east-northeast of the ARE2 site. As mentioned earlier, the basin land between the 2 locations was relatively flat, though lined to the west with jagged mountains that rose to about 8,000 ft, and a relatively level mountain ridge to the east that rose about 10,000 ft. To the northeast was a single mountain peak of 12,000 ft.

Image specifications from each of the sWSI images and the correlated sky observations were tabulated for future analyses. Individual images were preserved in an archive.

### **3.5 Sky/Cloud Data Processing**

---

One of the future usages for these images is to provide instructive resources for using machine learning techniques to derive predictive algorithms for solar radiation and/or power production, based on cloud types and amounts. In preparation for the machine learning, each image needed to be digitized. Consequently, a scheme was developed to communicate sky features using numbers. This method required overlaying a pre-sized grid onto the sWSI image. Each grid square was classified as either All Clouds, All Clear, Partial Cloud/Sky, Image Border with All Clouds/Clear Sky/Partial Cloud-Sky, Sun Glint, Sun and Glory with All Clouds/Clear Sky/Partial Cloud-Sky, or the background Black Border (see Table 1).

**Table 1 sWSI digitization categories examples**

<b>Number</b>	<b>Description</b>
10	All Clouds
00	All Clear
-10	Partial Cloud, Partial Sky
51	Image Border with All Clouds
50	Image Border with Clear Sky
-51	Image Border with Partial Cloud, Partial Sky
33	Sun Glint or Artifact of Photography in Cell
71	Sun and Glory in cell, with All Clouds Covering Sun
70	Sun and Glory in cell, with Clear Sky
-71	Sun and Glory in cell, with Partial Cloud, Partial Sky
99	Black Border

The manually entered assessment was then preserved in a file for machine learning input. A generic example of the digitized image results is presented in Fig. 6. Note that the image analysis is not a function of pixel type. It is the interpretation of what sky or lens feature is represented by the pixel, which is the goal. This added discriminatory layer is what has kept a “human in the loop” for this step of the postprocessing. With enough digitized data input, it is hoped that machine learning will ultimately replace the human-in-the-loop step.

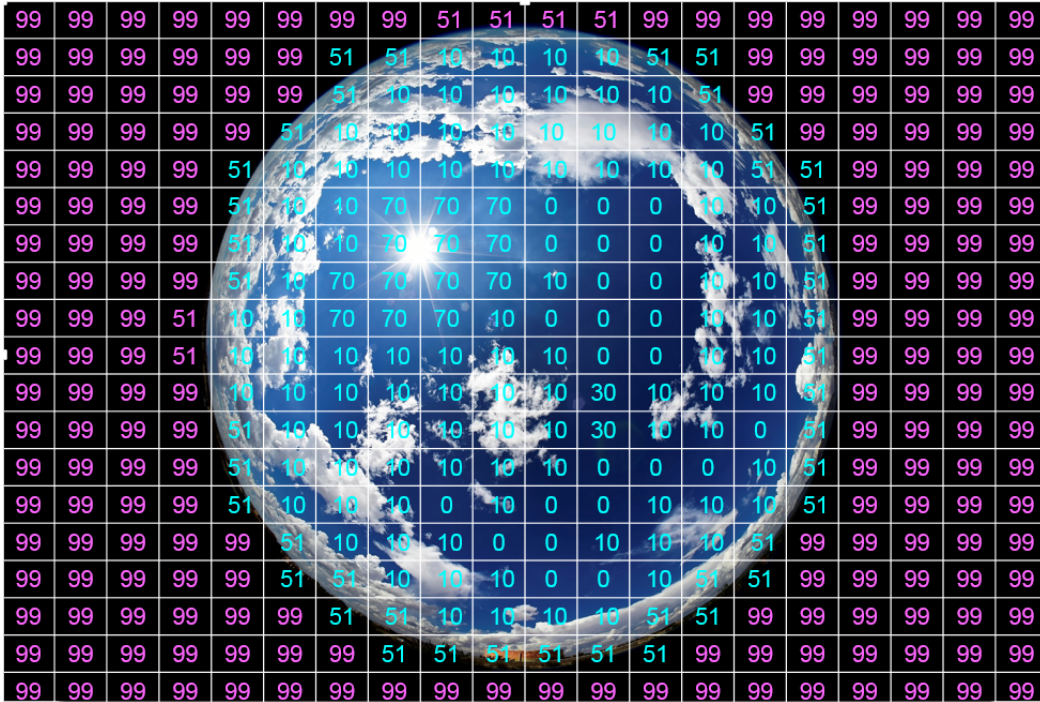


Fig. 6 sWSI digitization example

## 4. Results and Discussion

After 10 weeks of routine hourly cloud observations and manually evaluating a portion of the post-ARE2 sWSI image processing, repeated patterns within the sWSI images were noted and lessons learned were gleaned. Some of the more frequently observed features are listed in Section 4.1. The lessons learned are in Section 4.2.

### 4.1 Observations from the sWSI Data

Some of the more frequently observed features from the sWSI data include the following:

- Seasonal Cases Confirmed: In June 2017, there were little to no clouds in the sky. When the monsoon arrived in July 2017, clouds of various types populated the New Mexico sky.
- Overcast Case Studies: Some July morning skies started as overcast, which could be good post-ARE2 case study material.

- Cumulus Case Studies:
  - In June, the Cu clouds did not have much buildup. The buildup started to occur in July. There were numerous Cb clouds during July. A few occurred directly over the site.
  - In June, July, and August, Cu clouds repeatedly developed on the eastern horizon, near the tallest peak mountains.
  - Frequently, Cu clouds formed over the southwestern mountains in July.
- Haze: Near-surface haze cases were difficult to discern from just the postprocessing images.
- Lens Artifacts:
  - Solar Disc: When the sun was close to the horizons (morning and evening time periods), the solar disc appeared relatively small with respect to the solar disc seen during the midday hours.
  - Sun and Lens Glint: The locations of the sun and lens glint followed a distinct pattern. During the morning and evening hours, the sun and glint were far from each another. When the sun was on the eastern horizon, the glint was observed in the western part of the fov. By 1600 Local Time (LT), as the sun was approaching the western horizon, the glint was near the eastern horizon. During the midday hours, the sun and glint moved closer together, overlapping at 1300 LT.
  - Sun Glint and U-Glow (“array of the sun”): A “U-Glow” is an artifact of the fisheye lens that causes the sunlight to glow in a semicircle. The U-Glow generally only appeared between 1100 and 1600 LT. The glint and U-Glow had a relationship in that they were always opposite one another. The U-Glow generally initiated on the east side of the sun, while the glint was on the west side. When the U-Glow was observed on the west side of the sun, the glint would be on the east side. If the glint position was southwest of the sun, the U-Glow would be northeast of the sun.
  - Lens Reflection: In some of the 0800 LT west pyranometer platform images, a reflection appeared lower than the horizon. This reflection was only present during the morning hours, when the sun was close to the horizon. As soon as the sun gained elevation (~0900 MDT), the reflection disappeared.

## 4.2 Lessons Learned

---

1. Automating the sWSI Image Analyses: sWSI image analyses are not a function of just the pixel type (red, green, blue). It is the interpretation of what sky or lens feature is represented by the pixel that is the goal. This added discriminatory layer is what keeps a human in the loop for this step of the postprocessing. With enough digitized data input, however, it is hoped that machine learning will ultimately reduce the need for, or perhaps even replace, the human in the loop.
2. Analysis Challenges: There were times when 2 sWSI features overlapped within the same grid cell. For example, lens glint and U-Glow would overlap, or the sun overlapped with the border, or the sun overlapped with the glint. On a cloudy day, clouds and glint might overlap. There should be a special description for these situations. Here are 2 suggested solutions:
  - Option #1: Include both features. For example, if the sun and the border overlapped, enter “70/50” in the grid box.
  - Option #2: Combine the 2 features. For example, the description for the sun and border can be 750 (sun, border, and no clouds) and 751 (sun, border, and clouds)
3. Lens Artifacts (optical effects):
  - Lens flare, abnormal light areas in image: Lens flare and abnormal light areas in an image are caused by repeated reflections off of optical surfaces in the lens, with airspaces in between the lens elements. Light that encounters such surfaces will refract through the lens and reflect off the surfaces of subsequent elements, which reduces the amount of light that gets transmitted through the next element.
  - Lens flare is minimized when you multicoat all optical surfaces within the lens, which is composed of elements separated by airspaces. Such multicoating increases the refraction of light through the lens element and decreases the reflection off that same surface, thus decreasing the flare. A perfect multicoated lens will not produce flare.
  - Sun Star: A sun star is caused by light interacting with the rough/angled edges of the iris blades (of the F-stop diaphragm). To minimize the effect, the lens should have an increased number of diaphragm blades and be curved so that a perfect iris circle is made at all F-stops. The more circular the iris is, without rough edges between blades, the less points to the sun star. A perfect circle resolves into no sun star. A 10-pointed star comes from

a 5-bladed diaphragm. One can count the number of sun star points to figure out the number of blades in the optics diaphragm.

The shape of the lens flare (such as a pentagon), can also tell you how many diaphragm blades there are (and vice versa).

## **5. Conclusion and Recommendations**

---

ARE2 has produced a novel and detailed power, solar radiation, and cloud/sky documentation data set. The potential services provided by these data range from basic research seeking to investigate improved understanding of cloud impacts on solar radiation to practical application research that seeks to develop complex algorithms to empower diagnostic and predictive solar radiation tools tailored specifically for grid power production. This report was written to establish a common starting point for those seeking to use and exploit this data set. It is recommended that users of the data continue to document their findings so that the seeds planted by ARE2 can continue to grow into new understandings.

## 6. References

---

---

- Aerographer's Mate Third Class (Observer), Naval Education and Training Command, Rate Training Manual and Nonresident Career Course, Naval Education and Training Program Development Center; Pensacola, FL. Washington (DC): US Government Printing Office; 1984.
- Boxwell M. Solar electricity handbook, 2013 edition, a simple, practical guide to solar energy—designing and installing photovoltaic solar electric systems. Ryton on Dunsmore Warwickshire: Greenstream Publishing; 2009–2013.
- Haupt SE, Branko K, Jensen T, Lee J, Jimenez P, Lazo J, Cowie J, McCandless T, Pearson J, Weiner G, et al. The SunCast™ solar-power forecasting system: the results of the public-private-academic partnership to advance solar power forecasting. Boulder (CO): National Center for Atmospheric Research (NCAR), Research Applications Laboratory, Weather Systems and Assessment Program (US); 2016. NCAR Technical Note: NCAR/TN-562+STR.
- NIKON, Digital Camera D750 User's Manual. Nikon Corporation, 2014.
- NOAA/NWS and NASA Sky Watcher Chart. Silver Spring (MD): National Weather Service; 2015 [accessed 2017 Oct 27]. [https://www.weather.gov/media/owlie/skywatchers\\_chart.pdf](https://www.weather.gov/media/owlie/skywatchers_chart.pdf)
- Vaucher G. Atmospheric renewable-energy research, volume 1. White Sands Missile Range (NM): Army Research Laboratory (US); 2015 Sep. Report No.: ARL-TR-7402.
- Vaucher G. Atmospheric renewable energy research, volume 2: Assessment process for solar-powered meteorological applications. White Sands Missile Range (NM): Army Research Laboratory (US); 2016 Aug. Report No.: ARL-TR-7762.
- Vaucher G, Brice R, Luces S, O'Brien S. Local-Rapid Evaluation of Atmospheric Conditions (L-REACT™) System, design and development, volume 3: Operational L-REACT™. White Sands Missile Range (NM): Army Research Laboratory (US); 2011 Sep. Report No.: ARL-TR-5727.
- Vaucher G, Smith J, Berman M. Atmospheric renewable energy research, volume 3: solar-power microgrids and atmospheric influences. White Sands Missile Range (NM): Army Research Laboratory (US); 2016 Sep. Report No.: ARL-TR-7797.

## List of Symbols, Abbreviations, and Acronyms

---

24/7	24 h/d, 7 d/week
ArL	above roof level
ARL	US Army Research Laboratory
ARE	Atmospheric Renewable Energy
ARE1	Atmospheric Renewable Energy Field Study #1 (2016)
ARE2	Atmospheric Renewable Energy Field Study #2 (2017)
Ac	altocumulus
As	altostratus
Cb	cumulonimbus
Cc	cirrocumulus
Ci	cirrus
Cs	cirrostratus
Cu	cumulus
CD	compact disc
DAS	Data Acquisition System
DC	direct current
DGM	Distributed Grid Manager
DMBC	Distributed Model Based Control
fov	field of view
GPS	global positioning system
I	current
L-REAC	Local-Rapid Evaluation of Atmospheric Conditions
LT	Local Time
MDT	Mountain Daylight Time
MPPT	Maximum Power Point Tracking (Charge Controller)

Ns	nimbostratus
P	power
PV	photovoltaic
R	resistance
re	renewable energy
Sc	stratocumulus
St	stratus
sWSI	simulated Whole Sky Imager
V	voltage

1 DEFENSE TECHNICAL  
(PDF) INFORMATION CTR  
DTIC OCA

2 DIR ARL  
(PDF) IMAL HRA  
RECORDS MGMT  
RDRL DCL  
TECH LIB

1 GOVT PRINTG OFC  
(PDF) A MALHOTRA

17 DIR ARL  
(7 PDF, RDRL CIE D  
5 HC, G VAUCHER (5 CD, 5 HC)  
5 CD) S DARCY  
C HOCUT  
D KNAPP  
RDRL SED P  
M BERMAN  
D PORSCHE  
S HU

1 USMA  
(PDF) J FORRESTER

1 MISSISSIPPI VALLEY STATE UNIVERSITY  
(PDF) R YOUNG

1 CENTRAL STATE UNIVERSITY  
(PDF) M CURTICE

1 EMBRY RIDDLE AERONAUTICAL UNIVERSITY  
(PDF) C WALKER